Journal of Computational Science and Technology

Vol. 3, No. 1, 2009

Crystal Growth Prediction by First-Principles Calculations for Epitaxial Piezoelectric Thin Films*

Hwisim HWANG**, Yasutomo UETSUJI***, Sei-ichiro SAKATA ****, Kazuyoshi TSUCHIYA***** and Eiji NAKAMACHI**

**Faculty of Life and Medical Science, Doshisha University
1-3 Miyakodani, Tatara, Kyotanabe, Kyoto 610-0394, Japan
E-mail:emi1101@mail4.doshisha.ac.jp
*** Depatment of Mechanical Engineering, Osaka Institute of Technology
5-16-1, Omiya, Asahi-ku, Osaka, Osaka 535-8585, Japan
****Interdisciplinary Faculty of Science and Engineering, Shimane University
1060, Nishikawatsu-cho, Matsue, Shimane 690-8504, Japan
*****Department of Precision Engineering, Tokai University
1117, Kitakaname, Hiratsuka, Kanagawa 259-1292, Japan

Abstract

A numerical prediction scheme of crystal growth on various substrates by using the first-principles calculation was proposed to analyze the epitaxial processes of the piezoelectric thin films, such as the sputtering, the chemical vapor deposition and the molecular beam epitaxy processes. At first, we analyze the epitaxial strain of crystal cluster in piezoelectric thin film, which is caused by the lattice mismatch with the substrate. When the epitaxial strain is introduced in the unit cell of the crystal cluster, the total energy can be calculated by employing the pseudo-potential method based on the density functional theory. Then, a preferred orientation of crystal cluster is selected from the crystal conformations on the substrate which satisfy the structural stability condition. This numerical scheme was applied to $BaTiO_3$ thin films processes fabricated on various substrates, such as $SrTiO_3$(110), $SrTiO_3$(001), MgO(100) and $LaTiO_3$(001). Numerical results show that our process crystallographic design scheme, which employs the total energy increment of cluster, is efficient tool to evaluate the possibility of thin film crystal growth. Finally, it was confirmed that numerical results of preferred orientations have good correspondence with experimental ones.

Key words: First-Principle Calculation, Micromechanics, Piezoelectric Ceramics, Crystal Growth, Preferred Orientation, Lattice Mismatch

1. Introduction

Perovskite compounds, such as $BaTiO_3$ and $Pb(Zr,Ti)O_3$ (PZT), have a high piezoelectricity, which have a nonsymmetrical tetragonal crystal structure obtained through the phase transition from the cubic structure. This tetragonal crystal structure shows extreme anisotropies of mechanical and electrical properties. Consequently, the piezoelectric property depends strongly on the crystal orientation. Moreover, the perovskite compounds have the ferroelectricity, which is characterized by the domain switching that the *c*-axis direction of spontaneous polarization is switched by rotating angles of 90º or 180º caused by the external load. Recently, high performance piezoelectric thin films of perovskite compounds have been fabricated by using the sputtering [(1)], the chemical vapor

*Received 20 Oct., 2008 (No. T1-07-0908)
Japanese Original : Trans. Jpn. Soc. Mech. Eng., Vol.74, No.741, A (2008), pp.763-769 (Received 15 Oct, 2007)
[DOI: 10.1299/jcst.3.264]

deposition (CVD)[2] and the molecular beam epitaxy (MBE)[3]. These techniques enable us to control lattice parameters and crystal orientations of epitaxialy grown crystals on the various substrates. For examples, Zhu et al. fabricated [111]-oriented $BaTiO_3$ on $LaNiO_3$(111) substrate, which had a crystal orientation with maximum piezoelectric strain constant[4]. Nishida et al. fabricated [001] and [100]-orientated PZT thin films on MgO(001) substrate, and they succeeded to show a huge piezoelectric strain by synergetic effect of the piezoelectric strain of [001] orientation and the switching strain of [100] orientation under the external electric field[5]. Now, the demands of MEMS/NEMS actuators by using lead-free and biocompatible piezoelectric materials have expanded rapidly. Therefore, it is important to develop a practical and efficient numerical tool for epitaxial growth prediction and process design of thin-film fabrication on various substrates.

Until now, the conventional numerical methods, such as the molecular dynamics (MD) method and the first-principles calculation based on the density functional theory (DFT), have been applied to the crystal growth process simulations. In MD method, the reliability of its numerical results is poor, because of its uncertain inter-atomic potentials for the various combinations of several kinds of atoms. Only the applications to the pure metals succeeded, such as Ge growth on Si(111) substrate, obtained by Xu et al.[6]. In case of perovskite compounds, Paul et al. and Costa et al. analyzed the crystal structure transition caused by the stress and temperature increases[7], [8]. But it could not predict the differences of poly-crystal structures and material properties caused by changing combinations of the crystals and the substrates. Thus, the conventional MD method has many problems for the crystal growth prediction of perovskite compounds on the arbitrarily selected substrates.

On the other hand, DFT can treat interactions between electrons and protons, therefore the reliable inter-atomic potentials can be obtained. The DFT based first-principle calculations were applied to the epitaxial growth of the ferroelectric material, such as the study by Diegueaz et al. They evaluated the stress increase and the polarization by considering the lattice mismatch between a substrate and a thin film, such as $BaTiO_3$ and $PbTiO_3$[9]. Similarly, Yakovkin et al. had investigated in case of the $SrTiO_3$ thin film growth on the Si substrate[10]. However, these calculations adopted the assertive assumptions, such as fixing the conformations of thin film crystals and the growth orientations on the substrates. In this conventional algorithm, the grown orientation is determined by the purely geometrical lattice mismatch between thin films and substrates, so this algorism is not sufficient to predict accurately the preferred orientation of the thin film.

In this study, we propose the crystal growth prediction method by introducing the minimum assumption, such as ignoring the electron state transition on the substrates. Our scheme can be applied to the epitaxial growth process simulation and design of the piezoelectric thin film. The total energies of crystals with epitaxial strain are evaluated by using first-principles calculation under the condition that the crystal strains in the grown cluster are uniform. We evaluate the influences of the crystal strain on the total energy and the crystal growth potential on various substrates. Then we try to find a stabilized epitaxial growth of thin film crystal structure of $BaTiO_3$, which has a certain preferred orientation, on basis of the total energy estimation by using our first-principle calculations.

2. Crystal growth prediction by using the first-principles calculation

2.1 Evaluation method of total energy by using first-principles calculation

The tetragonal crystal structure of perovskite compound and its five typical orientations [001], [100], [110], [101] and [111] are shown in Fig.1. When the crystal cluster grows epitaxialy on a substrate, the lattice constants such as a, b, c, θ_{ab}, θ_{bc} and θ_{ca} are changed because of the lattice mismatch with the substrate. These crystal structure changes can be determined by considering six components of mechanical strain in crystallographic coordinate system such as ε_a, ε_b, ε_c, γ_{ab}, γ_{bc} and γ_{ca}. In general analysis procedure, the lattice

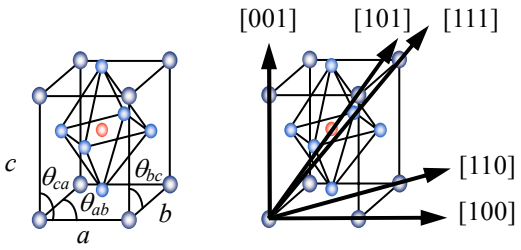

Fig.1 Crystal structure and orientations of perovskite compounds

mismatch in the specific direction was calculated and the crystal growth potential was derived. However, the epitaxialy grown thin film crystal is in a multi-axial state. Therefore, the numerical results of the crystal potential of thin films are not correct because of considering only uni-axis strain.

In this study, we evaluate the total energy of a crystal thin film with multi-axial crystal strain states by using the first-principles calculation, and apply to the case of the epitaxial growth process. An ultra-soft pseudo-potentials method is employed in DFT with the condition of LDA (Local Density Approximation) for exchange and correlation terms. The total energies of the thin film crystal as the function of six components of crystal strain are calculated to find a minimum value. Where, total energies are calculated discretely and a continuous function approximation is introduced. At first, a sampling area is selected by considering the symmetry between *a* and *b* axes in a tetragonal crystal structure. Secondly, sampling points are generated by LHS (Latin Hypercube Sampling) method[11], which is the efficient tool to get nonoverlap sampling points. Thirdly, a global function model is generated by KPHA (Kriging Polynomial Hybrid Approximation) method[12]. Next, a gradient of total energy at each sampling point is calculated and an approximate quadratic function is generated. Finally, the minimum point of a total energy can be found by using this function.

2.2 Crystal growth prediction method

We assume that several crystal unit cells of crystal clusters, which have certain conformations, can grow on a substrate as shown Fig.2. The left-hand side diagram in Fig.2 shows an example of conformation in cases of [001], [100], [110] and [101] orientations, and the right-hand side shows [111] orientation. O, A and B are points of substrate atoms corresponding to thin films ones within the allowable range of distance. l_{OA} and l_{OB} indicate distances of A and B from O, respectively. θ_{AOB} indicates the angle between lines OA and OB.

Table 1 summarizes the relationship between the lattice constants of thin film and l_{OA} and l_{OB} according to crystal orientations. Additionally, Table 1 shows crystal strains, which can be determined in the corresponded crystal orientations. But particular crystal strains, such as ε_i^* and γ_{ij}^*, can not be determined by employing the lattice constants of the thin

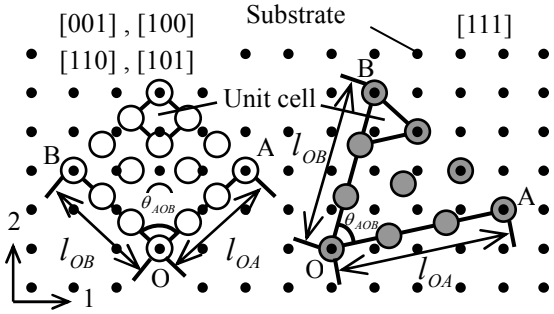

Fig.2 Schematic diagram of crystal conformations on a substrate

Table1 Relationship of lattice parameter and epitaxial strain with crystal orientations

	[001]	[100]	[110]	[101]	[111]
l_{OA}	a	c	c	$\sqrt{a^2+c^2}$	$\sqrt{a^2+c^2}$
l_{OB}	b	b	$\sqrt{a^2+b^2}$	b	$\sqrt{b^2+c^2}$
Epitaxial strain					
ε_a	$\frac{l_{OA}}{ka}-1$	ε_a^*	ε_a^*	ε_a^*	$\frac{\sqrt{(l_{OA}/k)^2-c^2(1+\varepsilon_c)^2}}{a}-1$
ε_b	$\frac{l_{OB}}{kb}-1$	$\frac{l_{OB}}{kb}-1$	$\frac{\sqrt{(l_{OB}/k)^2-a^2(1+\varepsilon_a^*)^2}}{b}-1$	$\frac{l_{OB}}{kb}-1$	$\frac{\sqrt{(l_{OB}/k)^2-c^2(1+\varepsilon_c)^2}}{b}-1$
ε_c	ε_c^*	$\frac{l_{OA}}{kc}-1$	$\frac{l_{OA}}{kc}-1$	$\frac{\sqrt{(l_{OA}/k)^2-a^2(1+\varepsilon_a^*)^2}}{c}-1$	$\frac{1}{ck}\sqrt{l_{OA}l_{OB}\cos\theta_{AOB}}-1$
γ_{ab}	$\theta_{AOB}-\theta_{ab}$	γ_{ab}^*	γ_{ab}^*	$\theta_{AOB}-\theta_{ab}$	γ_{ab}^*
γ_{bc}	γ_{bc}^*	γ_{bc}^*	$\theta_{AOB}-\theta_{bc}$	γ_{bc}^*	$\frac{b}{c}\gamma_{ab}^*$
γ_{ca}	γ_{ca}^*	$\theta_{AOB}-\theta_{ca}$	$\theta_{AOB}-\theta_{ca}$	$\frac{a}{c}\gamma_{ab}$	$\frac{a}{c}\gamma_{ab}^*$

ε_i^* and γ_{ij}^* can be given from first-principle calculation to minimize total energy.

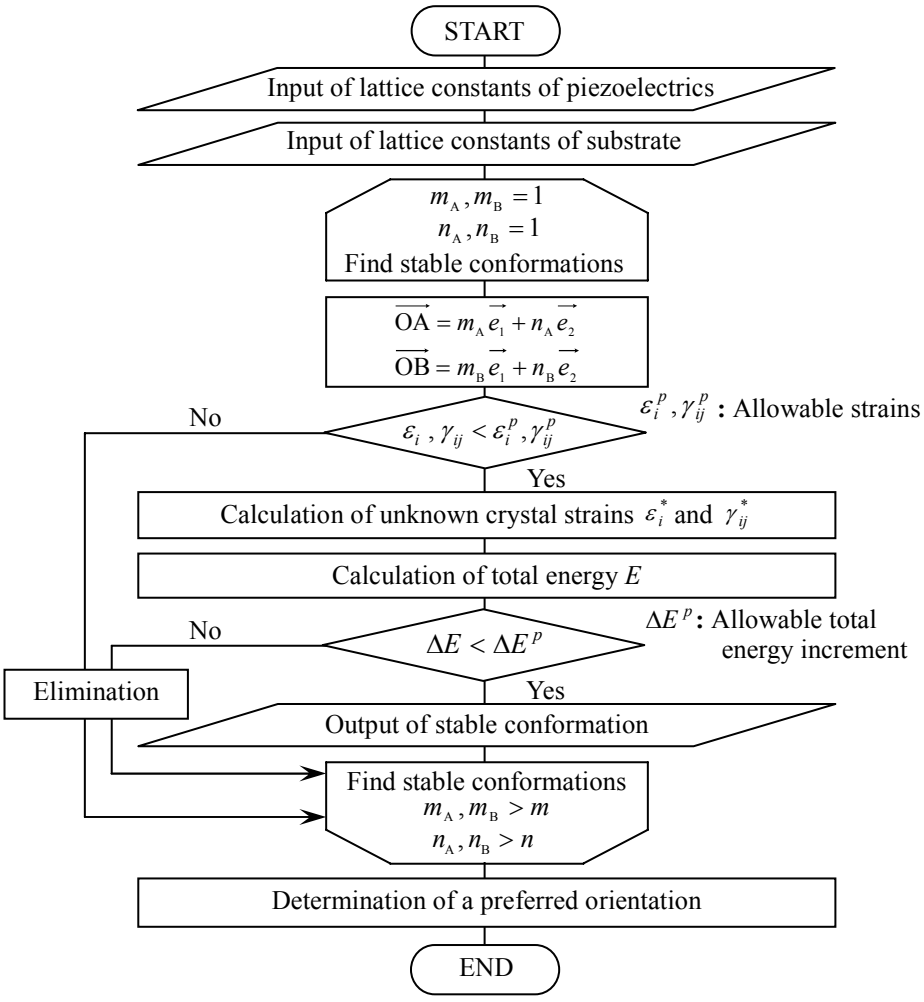

Fig.3 Flowchart of crystal growth prediction on basis of the first-principles calculations

film and the geometric constants of the substrate. In our calculation scheme, their unknown components are determined easily by employing the condition of minimum total energy of the crystal unit cell.

Figure 3 shows the flowchart of the crystal growth prediction algorithm. At first, lattice

constants of the thin film and the substrate are inputted. To generate candidate crystal clusters with assumed conformations and orientations. Substrate coordinates of A and B points, indicated as (m_A, n_A) and (m_B, n_B), are updated according to the calculation result under the condition of fixing O point. The search range of the crystal cluster is settled as $0 < m_A, m_B < m$ and $0 < n_A, n_B < n$ by considering the grain size of the piezoelectric thin film crystal. $\vec{e}_1$ and $\vec{e}_2$ as shown in Fig.3 are unit vectors of the substrate coordinate system. Lattice constants of the crystal cluster are compared with geometrical parameters of the substrate, and candidate crystal clusters, which have the extreme lattice mismatches, are eliminated. Crystal strains caused by the epitaxial growth are calculated for every candidates of the grown crystal cluster as shown in Table 1. Next, the total energy of grown crystal cluster is estimated by using the total energy as a function of crystal strains. Total energies of candidate crystal clusters are compared with one of the free-strained boundary condition. Then total energy increments of candidate crystal clusters are calculated. Finally, preferred orientations are determined in the corresponding crystal orientations, which have lower total energy increment than the allowable value.

3. Numerical results of $BaTiO_3$ thin film

3.1 Evaluation of total energies by using the first-principles calculation

Our prediction algorithm was applied to $BaTiO_3$ thin film crystal growth prediction on various substrates, and its availability was investigated through the comparison with the experiments. In this study, we evaluated the total energy by using the first-principles calculation. The **k**-point was used to sample the Brillouin zone with 8×8×8 meshes and 450eV for the cutoff energy. Lattice constants of the stable tetragonal structure of $BaTiO_3$, as a=b=0.3932nm and c=0.3972nm, were obtained. These lattice constants had -1.55% and -1.63% errors by comparison with the experimental values, as a=b=0.3992nm and c=0.4035nm, which were reported by B. Jaffe et al.[13].

Next, 40 sampling points of crystal strains were generated by LHS method within the range from -5.0% to +5.0%. The quadric approximation model was obtained by introducing KHPA method. To verify an accuracy of approximated total energy, the correct value of the first-principles calculation and the approximate values were compared for other arbitrary 10 sampling points produced by the LHS method. As a result, the maximum error between both values was confirmed to be 2.15×10^{-3}%. Consequently, the validity of this quadric approximation model based on the kriging method was confirmed to be an accurate prediction scheme because of its very low error in the local area.

Figure 4 shows the relationship between the normal strains ε_a, ε_b and the total energy under the condition of zero shear strain, where the normal strains ε_c were +5.0%, 0.0% and -5.0%. It shows that the approximate total energy indicates a minimum value at the zero strain state. When the crystal had compressive strains ε_a and ε_b, the total energy of the crystal with the tensile strain ε_c is the lows. In contrast, when the crystal had tensile strains ε_a and ε_b, the total energy of crystal with the compressive strain ε_c is the lows.

In order to verify the superiority of the crystal growth potential evaluation scheme by using the first-principles calculations, several total potential energies under the virtual strain states were compared. Table 2 shows the comparison of the total energies of various deformed crystals under the condition that the volumetric strain is zero. The total energy of the crystal under the condition of the tensile strains in the a and b axes and the compressive strain in the c axis was lower than ones under other conditions. Additionally, when the in-plane strains of a and b axes were difference, its total energy was higher than ones which had same in-plane strains.

Figure 5 shows the comparison of total energies in the growth directions under the condition of 1.0% epitaxial strain caused by the lattice mismatch on OA and OB lines. It

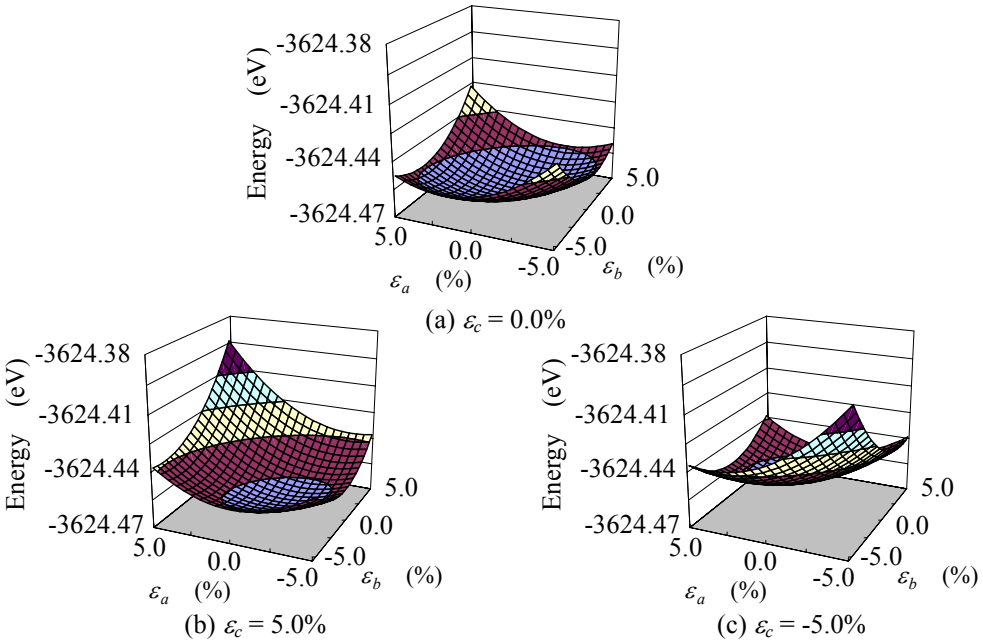

Fig.4 Energy elevation of perovskite-type $BaTiO_3$ by using the approximate energy function of crystal unit cell with respect to normal strains

Table2 Comparison of energy under some strain states without volumetric change by using the approximate energy function of crystal unit cell

No.	1	2	3	4
Deformation modes	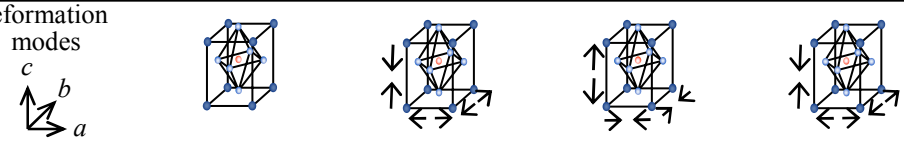			
ε_a (%)	0.00	0.50	-0.50	0.75
ε_b (%)	0.00	0.50	-0.50	0.25
ε_c (%)	0.00	-0.99	1.01	-0.99
$\gamma_{ab},\gamma_{ac},\gamma_{bc}$(%)	0.00	0.00	0.00	0.00
Energy (eV)	-3624.4699	-3624.4662	-3624.4661	-3624.4657
No.	5	6	7	
Deformation modes	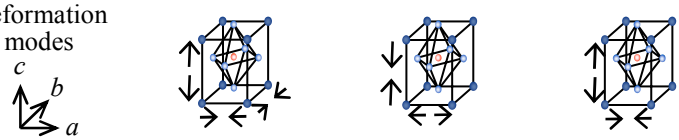			
ε_a (%)	-0.75	1.00	-1.00	
ε_b (%)	-0.25	0.00	0.00	
ε_c (%)	1.01	-0.99	1.01	
$\gamma_{ab},\gamma_{ac},\gamma_{bc}$(%)	0.00	0.00	0.00	
Energy (eV)	-3624.4656	-3624.4642	-3624.4641	

Orientation	[001]	[100]	[110]	[101]	[111]
ε_a	1.00	-0.74	1.02	0.66	-0.07
ε_b	1.00	1.00	0.98	1.00	-0.07
ε_c (%)	-1.05	1.00	1.00	1.33	2.03

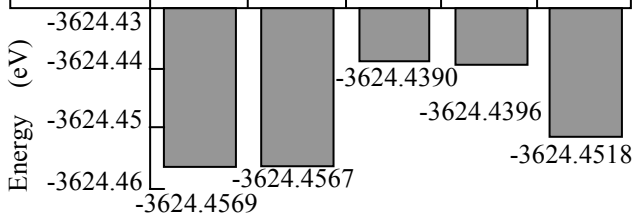

Fig.5 Comparison of energy among different crystal orientation under the same epitaxial strain

shows that if [001] and [100] orientations crystals grow on the substrate, the total energy show lowest value. It indicates that these orientations had a high crystal growth possibility. In contrast, [110] and [101] orientations have a high total energy and are difficult to grow on the substrate. Finally, it is confirmed that the difference of the growth potential among various crystal orientations can be evaluated by using the first-principles calculation under the condition of the epitaxial strain with the lattice mismatch.

3.2 Prediction of crystal growth process on various substrates

$BaTiO_3$ thin films crystals with various preferred orientations were fabricated on the substrates. These experimental results were listed in Table 3. In case of $SrTiO_3$ substrate, [110] orientation has grown on (110) face, and [001] and [100] orientations on (001) plane. [001] orientation has grown on the substrate crystal planes of MgO(100) and $LaNiO_3$(001).

Numerical results of our newly proposed analysis scheme as a process crystallography procedure to predict the crystal growth on the substrates were compared with the experimental results. Lattice parameters of $SrTiO_3$ with the perovskite cubic structure was set as a=b=c=0.3905nm. Table 4 shows the crystal structure in case of $SrTiO_3$(110), and Table 5 shows in case of $SrTiO_3$(001). The lattice parameter of MgO with the rocksalt cubic structure was set as a=b=c=0.4210nm and $LaNiO_3$ with the perovskite cubic was set as a=b=c=0.3840nm. Table 6 shows the numerical result of MgO(100), and Table 7 $LaTiO_3$(001). These tables indicate the grown crystal orientations, conformations of the grown crystal cluster, epitaxial strains, the total energies of the crystal unit cell and total energy increments of the crystal cluster. These tables show three candidates of the crystal cluster, which had lowest total energy increment. If we employed the threshold value of the total energy $\Delta E \le 0.06\,\mathrm{eV}$, the preferred orientations agreed well with experimental results as shown in Table 3. In case of conventional algorism, which based on the purely geometrical lattice mismatch, preferred orientations of $BaTiO_3$ on $SrTiO_3$(001) and $LaNiO_3$(001) have good agreements with experimental results, but MgO(100) and $SrTiO_3$(110) did not coincide.

In this section, we confirmed that our newly proposed scheme could predict accurately the epitaxial process of the piezoelectric thin film, and it was useful tool to design the piezoelectric thin film.

Table3 Experimental results for preferred orientations of $BaTiO_3$ thin films on various substrates

Substrate	Crystal face	Preferred orientation
$SrTiO_3$	(110) [a]	[110]
	(001) [b]	[001] , [100]
MgO	(100) [c]	[001]
$LaNiO_3$	(001) [d]	

[a] Ref.(14), [b] Ref.(15), [c] Ref.(16), [d] Ref.(4)

Table 4 Computational result for stable conformations and preferred orientations of $BaTiO_3$ thin film on $SrTiO_3$(110) substrate

Orientation	[110]	[101]	[110]
Model	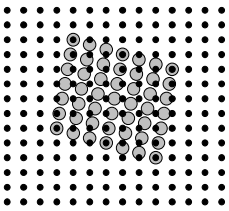	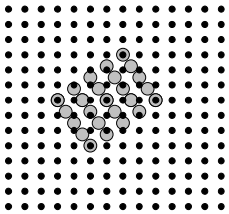	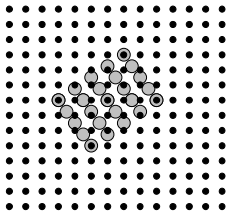
Epitaxial strain (%)	ε_a : 0.80 , ε_b : 0.10 ε_c : -0.64 , γ_{ab} : 0.00 γ_{ac} : 0.00 , γ_{bc} : 0.00	ε_a : 0.25, ε_b : 0.78 ε_c : -0.89 , γ_{ab} : 0.00 γ_{ac} : 0.00 , γ_{bc} : 0.00	ε_a : 1.15, ε_b : 0.41 ε_c : -0.32 , γ_{ab} : 0.00 γ_{ac} : 0.00 , γ_{bc} : 0.00
Energy of unit cell (eV)	-3624.4691	-3624.4661	-3624.4656
Total ΔE (eV)	0.0151	0.0615	0.0681

Table 5 Computational result for stable conformations and preferred orientations of $BaTiO_3$ thin film on $SrTiO_3$(001) substrate

Orientation	[001]	[100]	[001]
Model	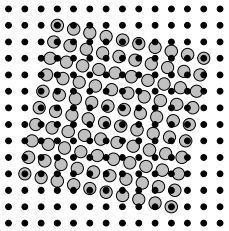	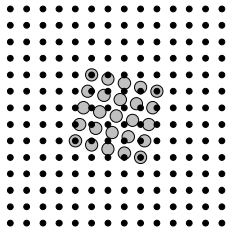	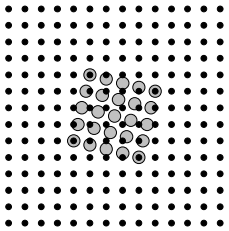
Epitaxial strain (%)	ε_a : 0.16, ε_b : 0.16 ε_c : -0.15 , γ_{ab} : 0.00 γ_{ac} : 0.00 , γ_{bc} : 0.00	ε_a : 0.25, ε_b : 0.78 ε_c : -0.32 , γ_{ab} : 0.00 γ_{ac} : 0.00 , γ_{bc} : 0.00	ε_a : 0.78, ε_b : 0.78 ε_c : -0.80 , γ_{ab} : 0.00 γ_{ac} : 0.00 , γ_{bc} : 0.00
Energy of unit cell (eV)	-3624.4693	-3624.4663	-3624.4659
Total ΔE (eV)	0.0582	0.0590	0.0665

Table 6 Computational result for stable conformations and preferred orientations of $BaTiO_3$ thin film on MgO(100) substrate

Orientation	[001]	[001]	[100]
Model	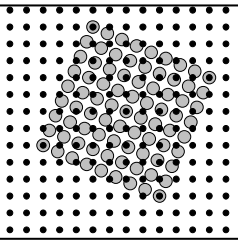	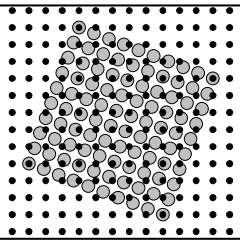	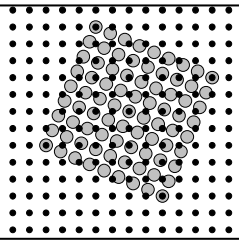
Epitaxial strain (%)	ε_a : 0.35, ε_b : 0.35 ε_c : -0.35 , γ_{ab} : 0.00 γ_{ac} : 0.00 , γ_{bc} : 0.00	ε_a : 0.07, ε_b : 0.07 ε_c : -0.05 , γ_{ab} : 0.00 γ_{ac} : 0.00 , γ_{bc} : 0.00	ε_a : 0.60, ε_b : 0.35 ε_c : -0.75 , γ_{ab} : 0.00 γ_{ac} : 0.00 , γ_{bc} : 0.00
Energy of unit cell (eV)	-3624.4692	-3624.4693	-3624.4689
Total ΔE (eV)	0.0463	0.0486	0.0646

Table 7 Computational result for stable conformations and preferred orientations of $BaTiO_3$ thin film on $LaNiO_3$(001) substrate

Orientation	[001]	[101]	[110]
Model	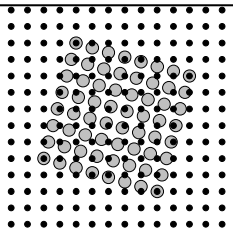	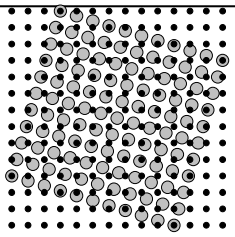	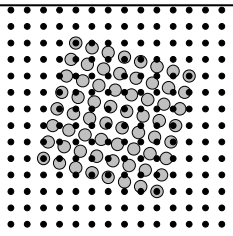
Epitaxial strain (%)	ε_a : -0.01, ε_b : -0.01 ε_c : 0.00 , γ_{ab} : 0.00 γ_{ac} : 0.00 , γ_{bc} : 0.00	ε_a : 0.38, ε_b : 0.38 ε_c : -0.40 , γ_{ab} : 0.00 γ_{ac} : 0.00 , γ_{bc} : 0.00	ε_a : 0.85, ε_b : -0.01 ε_c : -1.10 , γ_{ab} : 0.00 γ_{ac} : 0.00 , γ_{bc} : 0.00
Energy of unit cell (eV)	-3624.4696	-3624.4691	-3624.4678
Total ΔE (eV)	0.0147	0.0821	0.1030

4. Conclusion

In this study, we proposed the numerical prediction scheme of the epitaxialy grown piezoelectric crystal thin film based on the process crystallography theory. It was applied to the piezoelectric material $BaTiO_3$, where the total energy of $BaTiO_3$ crystal was evaluated by using the first-principle calculation and the crystal growth process on various substrates was analyzed.

The numerical results suggest that there is a high dependency of the total energy on the orientation of the grown cluster. Then a high accuracy evaluation scheme is strongly required for the grown thin film crystal on the various substrates by using the total energy of crystal with the epitaxial strain caused by the lattice mismatch between a thin film and a

substrate.

We employed the threshold value of the total energy to determine the candidate grown cluster, and we proved that a crystal cluster, which had lower total energy than the threshold value, grew on a substrate through the comparison with the experimental results. Numerical results of preferred orientations, which were fabricated on $SrTiO_3$(110) and (001), MgO(100) and $LaNiO_3$(001), have shown good agreements with experimental ones. Consequently, we confirmed that our numerical scheme could predict the epitaxial process of the piezoelectric thin film efficiently and it was a powerful analysis tool to design the new piezoelectric thin film.

Acknowledgment

This work was financially supported by a Grant-in-Aid for Young Scientists (B) [No.19760080] from the Ministry of Education, Culture, Sports, Science and Technology of Japan.

References

(1) Kanno, I., Kottera, H., Matsunaga, T. and Wasa, K., Crystalline Structure of Epitaxial Pb(Zr,Ti)O_3 Thin Films, *Journal of Applied Physics*, Vol.97 (2005), pp.074101.1-074101.5.

(2) Tohma, T., Masumoto, H. and Goto, T. , Preparation of $BaTiO_3$-$BaZrO_3$ Films by Metal-Organic Chemical Vapor Deposition, *Japanese Journal of Applied Physics Part1*, Vol.41, No.11B (2002), pp.6643-6646.

(3) Yoneda, Y., Okabe, T., Sakaue, K., Terauchi, H., Kasatani, H. and Deguchi, K., Structural Characterization of $BaTiO_3$ Thin Films Grown by Molecular Beam Epitaxy, *Journal of Applied Physics*, Vol.83, No.5 (1998), pp.2458-2461.

(4) Zhu, J., Zheng, L., Luo, W. B., Li, Y. R. and Zhang, Y., Microstructural and Electrical Properties of $BaTiO_3$ Epitaxial Films on $SrTiO_3$ Substructures with a $LaNiO_3$ Conductive Layer as a Template, *Journal of Physics , Series D,* Vol.39 (2006), pp.2438-2443.

(5) Nishida, K., Wada, S., Okamoto, S., Ueno, R., Funakubo, H. and Katoda, T., Domain Distributions in Tetragonal Pb(Zr,Ti)O_3 Thin Films Probed by Polarized Raman Spectroscopy, *Applied Physics Letters*, Vol.87 (2005), pp.232902-1-232902-3.

(6) Xu, J. L. and Feng, J. Y., Study of Ge Epitaxial Growth on Si Substrates by Cluster Beam Deposition, *Journal of Crystal Growth*, Vol.240, No.3 (2002), pp.407-404.

(7) Paul, J., Nishimatsu, T., Kawazoe, Y. and Waghmare, U. V., Ferroelectric Phase Transitions in Ultrathin Films of $BaTiO_3$, *Physical Review Letters*, Vol.99, No.7 (2007), pp.077601-1-077601-4.

(8) Costa, S. C., Pizani, P. S., Rino, J. P. and Borges, D. S., Structural Phase Transition and Dynamical Properties of $PbTiO_3$ Simulated by Molecular Dynamics, *Journal of Condensed Matter*, Vol.75, No.6 (2006), pp.064602-1-064602-5.

(9) Dieguez, O., Rabe, K., M. and Vanderbilt, D., First-Principles Study of Epitaxial Strain in Perovskites, *Physical Review, Series B*, Vol.72, No.14 (2005), pp.144101-1-144101-9.

(10) Yakovkin, I. N. and Gutowski, M., $SrTiO_3$/Si(001) Epitaxial Interface: A Density Functional Theory Study, *Physical Review, Series B*, Vol.70, No.16 (2004), pp.165319-1-165319-7.

(11) Olsson, A. M. J. and Sandberg, G. E., Latin Hypercube Sampling for Stochastic Finite Element Analysis, *Journal of Engineering Mechanics*, Vol.128, No.1 (2002), pp.121-125.

(12) Sakata, S., Ashida, F. and Zako, M., Hybrid Approximation Algorithm with Kriging and Quadratic Polynomial-based Approach for Approximate Optimization, *International Journal for Numerical Methods in Engineering*, Vol.70, No.6 (2007), pp.631-654.

(13) Jaffe, B., Cook Jr., W. R. and Jaffe, H., *Piezoelectric Ceramics*, (1971), pp.54, Academic Press Inc.
(14) Iijima, K., Yamamoto K. and Hirata K., Preparation of Ferroelectric $BaTiO_3$ Thin Films by Activated Reactive Evaporation, *Applied Physics Letter*, Vol.56, No.6 (1990), pp.527-529.
(15) Li, C.L., Chen, Z. H., Zhou, Y. L. and Cui, D. F., Effect of Oxygen Content on the Dielectric and Ferroelectric Properties of Laser-Deposited $BaTiO_3$ Thin Films, *Journal of Physics Condens Matter*, Vol.13 (2001), pp.5261-5268.
(16) Murphy, T. E., Chen, D. and Phillips, J. D., Electronic Properties of Ferroelectric $BaTiO_3$/MgO Capacitors on GaAs, *Applied Physics Letters*, Vol.85, No.15 (2004), pp.3208-3210.